

STUDIES OF A GENERALIZED BEAM-INDUCED MULTIPACTING RESONANCE CONDITION*

K.C. Harkay[†], L. Loiacono[‡], and R.A. Rosenberg,
 Argonne National Laboratory, Argonne, IL, 60439, USA
[‡] Loyola University, Chicago, IL, 60611, USA

Abstract

At certain bunch intensities and bunch spacings, beam-induced multipacting (BIM) was observed during experiments performed at the Advanced Photon Source. Dedicated diagnostics known as retarding-field analyzers (RFAs) were used to directly measure the electron flux on the vacuum chamber walls. The peak signals were observed at a bunch spacing other than that predicted in the classical form of BIM, which assumes cold secondary electron emission. Using a simple computer model, we studied the effect of including an energy distribution for the emitted secondary electrons. We found that the experimental data can be explained by a resonance condition in which the secondary electron energy and surface emissivity properties are included. Results for positron beams are presented.

INTRODUCTION

Experiments were carried out in the 7-GeV Advanced Photon Source third-generation x-ray light source using dedicated diagnostics to measure the properties of the background, low-energy electron cloud [1]. The diagnostic is based on the planar retarding-field analyzer (RFA) [2], and both the time-averaged flux and energy spectrum were measured for electrons striking the vacuum chamber wall for varying machine conditions. A main goal of the experiments was to acquire data to provide realistic limits on key parameters relating to electron-cloud production, improving the predictive capabilities of computer models. The electron cloud was very sensitive to the bunch intensity and spacing. Maximum amplification for positrons was observed for bunches spaced at 7λ (20 ns), where λ is the rf wavelength. The enhancement was clearly seen for bunch intensities above 1.5 mA (5.5 nC).

These experimental results were compared with the code POSINST, developed by M. Furman and M. Pivi. The position of the peak and width of the resonance curve (RFA signal vs. bunch spacing) were found to be sensitive to the secondary electron energy (SEE) [3,4]. In the code, the distribution assumes the form: $E \exp(-E/E_s)$, where E_s is a constant. Good agreement was found for $E_s = 1$ eV.

If secondary electron emission processes dominate, the electron cloud can build up significantly if a BIM resonance condition is satisfied. In its classical form [5], cold electrons at the wall are accelerated by the beam and traverse the chamber in precisely the time between bunch passages. It was noted by M. Furman [3] that the range of

bunch spacings over which amplification was observed for APS positrons (4λ to 16λ) is consistent with the classical BIM condition for trajectories ranging between the minor and major chamber axes. However, the cold electron assumption is clearly incomplete, since the peak at 7λ cannot be readily explained. M. Furman and S. Heifets proposed a general BIM resonance that includes a non-zero SEE; this general form of BIM appeared to explain the data [1]. A simple computer model was written in order to study the dependence of the general BIM resonance condition on the emitted SEE. The model is described and the results are compared with the APS experimental data.

MODEL

The interaction between an electron and a train of bunches is modeled as a series of drifts and instantaneous kicks. The electron is constrained to move on a trajectory that crosses the chamber center. In the “impulse kick” approximation [5], the electron momentum gain is given by $\Delta\mathbf{p} = m_e c r_e N_b / r \hat{\mathbf{r}}$, where m_e is the electron mass, c is the speed of light, $r_e = 2.82 \times 10^{-13}$ cm is the classical electron radius, N_b is the bunch population, and r is the distance between the electron and the bunch. $\hat{\mathbf{r}}$ is a unit vector pointing towards a positron beam and away from an electron beam. Between bunch passages, the electron drifts under its momentum. If the electron strikes the wall before the next kick, a secondary electron is created with a nonzero energy and assumed to drift towards the beam. At the next kick, the electron’s new position is calculated, and its new momentum is given by $\mathbf{p} = \Delta\mathbf{p} + \mathbf{p}_0$, where \mathbf{p}_0 is the momentum just prior to the kick.

For improved accuracy, since it is not exactly an ellipse, the APS vacuum chamber shape was modeled according to design drawings. The chamber schematic is shown in Fig. 1, where θ is an angle measured from the vertical. The available path length for a given electron will vary according to θ . The mounted RFA position is between 49 and 67 deg. The antechamber (between 80 and 90 deg) was not taken into account in the model.

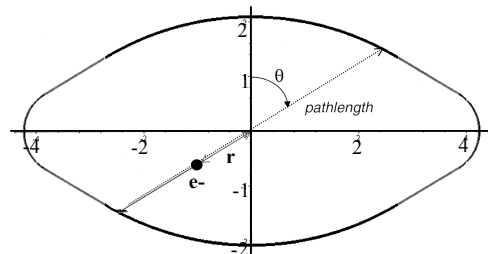


Figure 1: Vacuum chamber geometry used in the model. The chamber half-dimensions are 4.25×2.1 cm.

* Work supported by the U.S. Department of Energy, Office of Basic Energy Sciences under Contract No. W-31-109-ENG-38.

[†] harkay@aps.anl.gov

At a given bunch spacing, an electron with initial $(r_0, \theta, \mathbf{p}_0)$ is tracked for N kicks, and its new (r, \mathbf{p}) are recorded for each kick (θ is constant). The calculations are repeated for a range of values of θ and SEE. The output is checked for a resonance condition as follows: If the electron energies on three successive kicks are within 0.5 eV of each other, the resonant values of (r, θ, \mathbf{p}) , SEE, and kick details are recorded. The secondary emission at resonance depends on the electron incident energy $KE = \mathbf{p}^2/2m_e$. The secondary electron yield coefficient $\delta(KE)$ corresponding to the resonant condition is also recorded.

Input Parameters

δ is a critical input parameter. Figure 2 shows the values of δ measured as a function of incident electron energy for a APS aluminum chamber sample [6]. If δ is greater than unity for the resonant electron striking the walls, amplification can occur. The measured energy dependence of the data very nearly fits the universal δ curve for true secondary electrons, using an empirical formula developed by Furman [7]. The maximum value of δ occurs at $\delta_{max} = 2.8$ for an incident energy $E_{max} = 330$ eV. It should be noted that there was ~10% variation in δ_{max} among the measured samples.

The final resonant energy is not sensitive to the electron starting position and energy, but the number of kicks before falling into resonance is. The most probable “seed” electron is a secondary created at the wall. Rather than use a secondary electron (SE) distribution from the literature, we used the APS data [1] to choose an initial SEE that is near the mean value. We differentiated the RFA signal for a case where the bunches were far apart: 128λ (360 ns)

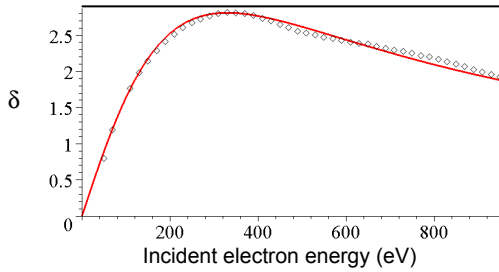


Figure 2: Measured secondary-electron yield coefficient δ for Al APS chambers, fitted to empirical formula in [7].

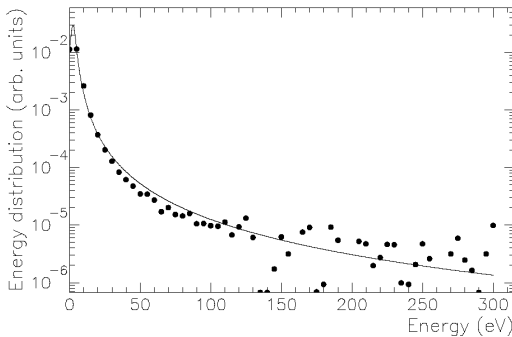


Figure 3: Measured electron-cloud energy distribution fitted with a Lorentzian function (data for 10 positron bunches spaced at 128λ , with 2 mA (7.4 nC) per bunch).

(see Fig. 3). In this case, there is no electron amplification. A Lorentzian function, $(\Gamma/2)/\{(\Gamma/2)^2 + (E - \langle E \rangle)^2\}$, fits the data well, where the width Γ is 4 eV and the mean (most probable) energy $\langle E \rangle$ is 2.5 eV. For this distribution, 90% of the SEs are within 10 eV, and about 50% are within $\langle E \rangle \pm \Gamma/3$ (i.e., SEEs ranging from 1.2 to 3.8 eV). Note the Lorentzian tail falls off more slowly than the exponential function assumed in POSINST.

RESULTS

Calculations of resonance conditions for a range of SEEs comprising 50% of the distribution were performed for bunch spacings ranging from 4 to 9λ . The bunch intensity is 2 mA to compare with the experimental data. In the examples shown in Figs. 4 and 5, the bunch spacing is 7λ . In Fig. 4, the resonant electron energy after 50 kicks is shown as a function of SEE at two angles: 0 deg (vertical plane) and 56 deg (RFA location). The inset in the figure shows the kinetic energy as a function of kick number for SEE = 2.5 eV. The resonance is reached after about 5-10 and 10-20 kicks for 0 and 56 deg, respectively. In the vertical plane, the resonant energy is 10 keV or more for SEEs between 2.9 and 3.7 eV. For these cases, the resonant condition corresponds to an electron position

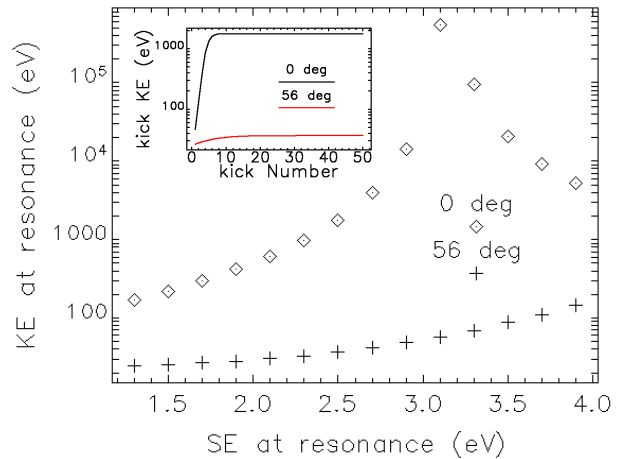


Figure 4: Resonant energy of an electron after 50 kicks for a range of SEEs (a) in the vertical plane (0 deg) and (b) at the location of the RFA (56 deg).

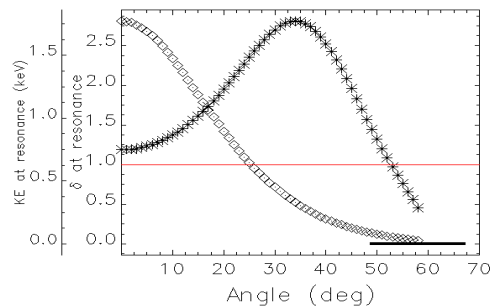


Figure 5: Electron kinetic energy (\diamond) and δ ($*$) at resonance as a function of the angle θ ; the SEE is 2.5 eV. The RFA location is represented by the thick line.

r that is very close to the beam. Here, the energy gain is likely to be overestimated by the impulse kick approximation. This is because the bunches are no longer short ($\sigma_z \approx 30 c$ ps) compared to the electron drift distance during the bunch passage. In these cases, δ is negligible and these resonances do not contribute to the electron cloud.

In Fig. 5, the resonance conditions are shown as a function of angular position θ for an SEE of 2.5 eV, showing the electron kinetic energy and corresponding δ . There are no resonances for $\theta > 60$ deg; this includes part of the RFA area. However, δ is greater than unity for angles up to just past the edge of the RFA.

The full space of resonance solutions in (r, θ) are shown graphically in Fig. 6 for different bunch spacing values. The δ corresponding to each resonance is marked in color. It can be seen that while few resonances exist for 4λ , a successively larger area is resonant up to 7λ , after which the area diminishes. Notably, 7λ has the largest area of resonances corresponding to $\delta \geq 2.0$, followed by 6λ . This is consistent with the experimental data, and could help explain the strong peak at 7λ [1]. There were no resonance solutions for $1-3 \lambda$ in this range of SEEs.

The results shown in Fig. 6 suggest that since the solutions were found using secondary electrons starting from the wall, it is likely that electrons will populate these regions in the chamber after 5-20 bunches (from Fig. 4). Synchrotron radiation reflecting from the chamber surfaces above and below the antechamber (not show, 0.5 cm half height) can strike virtually anywhere on the surface, producing both photoelectrons and secondary electrons. Interestingly, in the simulations for the APS at $7\text{-}\lambda$ bunch spacing using POSINST, a snapshot of the electron cloud spatial distribution after the 9th bunch passage shows a clumping of electrons in a region approximately in agreement with Fig 6 [3].

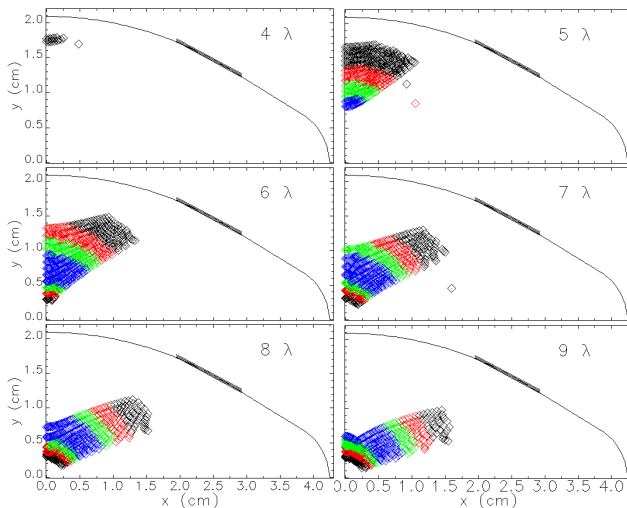


Figure 6: Resonance conditions as a function of bunch spacing for SEE between 1.2 and 3.8 eV. The color legend is: $1.0 \leq \delta < 1.5$ (black), $1.5 \leq \delta < 2.0$ (red), $2.0 \leq \delta < 2.5$ (green), and $2.5 \leq \delta$ (blue).

Verification of Cold Electron Model

We verified that the model gives the expected result in the limit that the secondary emitted electrons have zero energies. In Fig. 7, the positions of the resonant conditions for a bunch spacing of 4λ are shown, assuming that the SEE ≤ 0.1 eV (2 mA/bunch). As expected, only the electrons at the wall near 0 deg satisfy the BIM resonance. Figures 6 and 7 show that the area in the chamber covered by resonantly multipacting electrons is significantly underestimated by the cold secondary-electron BIM model.

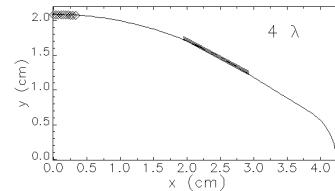


Figure 7: Resonance conditions for $4\text{-}\lambda$ bunch spacing for SEE ≤ 0.1 eV. The corresponding δ is ~ 0.7 .

CONCLUSIONS/FUTURE WORK

A simple computer model was written to study the dependence of a general beam-induced multipacting resonance condition on the secondary electron energy distribution. The results are consistent with the experimental data at the APS and help explain the peak observed in the electron cloud signal at a bunch spacing of 7λ (20 ns). Preliminary modeling has been performed for electron beams (currently in operation) and will be presented in the future. Of recent interest is a possible installation in the APS of a superconducting (SC) undulator. The heat deposition from electron bombardment is being analyzed. Also planned is modifying the model to allow different chamber dimensions; e.g., for the SC undulator chamber and other rings. In addition, a more realistic, nonimpulse kick will be implemented, taking the bunch longitudinal profile into account, as suggested in [8].

REFERENCES

- [1] K.C. Harkay and R.A. Rosenberg, Phys. Rev. ST Accel. Beams **6**, 034402 (2003).
- [2] R.A. Rosenberg and K.C. Harkay, Nucl. Instrum. Methods A **453**, 507 (2000).
- [3] M.A. Furman, M. Pivi, K.C. Harkay and R.A. Rosenberg, Proc. 2001 PAC, 679 (2001).
- [4] K.C. Harkay, R.A. Rosenberg, M.A. Furman, M. Pivi, Proc. of Mini-Workshop on Electron-Cloud Simulations for Positron and Proton Beams, CERN Yellow Report No. CERN-2002-001, 69 (Apr. 2002).
- [5] O. Gröbner, Proc. 10th Int'l. Conf. on High-Energy Accel., Protvino, 277 (1977); Proc. of 1997 PAC, 3589 (1997).
- [6] R.A. Rosenberg et al., to be published in J. Vac. Sci. Technol., (2003).
- [7] M.A. Furman and M.T.F. Pivi, Phys. Rev. ST Accel. Beams **5**, 124404 (2002).
- [8] J.S. Berg, LHC Project Note 97, CERN (1997).